TÜBİTAK

Turkish Journal of Chemistry

http://journals.tubitak.gov.tr/chem/

Research Article

Turk J Chem
(2015) 39: 984 – 997

doi:10.3906/kim-1504-2

Thermogravimetric analysis-based screening of metal (II) chlorides as dopants for the destabilization of solid-state hydrazine borane

Weiguang CHEN, Ümit Bilge DEMİRCİ*
Institut Européen des Membranes, University of Montpellier, Montpellier, France

Received: 02.04.2015 • **Accepted/Published Online:** 08.06.2015 • **Printed:** 30.10.2015

Abstract: Thermogravimetric analysis (TGA) is a powerful technique for screening boranes envisaged for chemical hydrogen storage. The demonstration is based on the use of six metal (II) chlorides (MCl_2) (with M as 3d-metal or d^8-metal) as destabilizing agents of solid-state hydrazine borane ($N_2H_4BH_3$). On the basis of TGA profiles combined with derivative thermogravimetric (DTG) curves, it is shown that: e.g. (1) $CuCl_2$ is an inefficient dopant whereas it is efficient towards ammonia borane (NH_3BH_3); (2) one of the best destabilization results is achieved with $N_2H_4BH_3$ doped by 10 wt% $CuCl_2$-$NiCl_2$, the sample decomposing from 30 °C with greatly mitigated amounts of gaseous by-products; (3) in a few cases, the destabilization extent is so important that the doped samples could be envisaged as energetic materials. Above all, the present report shows the importance of TGA-DTG in the field of boron- and nitrogen-containing materials and the proposed protocol could be used by other groups so that literature-based comparisons are more relevant.

Key words: Hydrazine borane, metal chloride, screening, thermogravimetric analysis, thermolysis

1. Introduction

Boron- and nitrogen-containing materials have been the objects of intense research over the past 10 years owing to some attractive features: presence of both hydridic $H^{\delta-}$ and protic $H^{\delta+}$ hydrogens in the same molecule, low density (<1 g cm^{-3}), high gravimetric and volumetric hydrogen storage capacities, and relative thermal stability.[1−3] A typical example, also the most investigated to date, is ammonia borane (NH_3BH_3): 3 $H^{\delta-}$ and 3 $H^{\delta+}$; 0.78 g cm^{-3}; 19.5 wt% H and 146 g(H) L^{-1}; and stable under heating (at constant heating rate) up to ca. 100 °C.[4−6] Accordingly, ammonia borane and, more widely, boron- and nitrogen-containing materials have been considered as potential solid-state chemical hydrogen storage materials, and the main objective has been to destabilize the compound so that it liberates pure hydrogen at temperatures lower than 100 °C.

Hydrazine borane ($N_2H_4BH_3$) (0.98 g cm^{-3}) is another example of hydrogen-dense boron- and nitrogen-containing materials: i.e. with 3 $H^{\delta-}$ and 4 $H^{\delta+}$, hydrogen storage capacities of 15.3 wt% H and 149 g(H) L^{-1}, and stability under heating up to ca. 60 °C.[7] Discovered in the 1960s,[8] it was first found to be suitable as solid-state monopropellant for rocketry and fast hydrogen generating systems.[9] More recently, it was suggested to be a possible candidate for chemical hydrogen storage,[10] provided it is not used in pristine state.[7] Indeed, better dehydrogenation performance, in terms of onset temperature of reaction and release of unwanted gaseous side-products, can be obtained by adding a destabilizing agent (e.g., LiH, $LiBH_4$, NH_3BH_3),[11−13] or by

*Correspondence: umit.demirci@um2.fr

chemically modifying the borane to form hydrazinidoborane derivatives (e.g., $LiN_2H_3BH_3$, $NaN_2H_3BH_3$, $KN_2H_3BH_3$).[14–16] Improved dehydrogenation performance could be also achieved with other destabilizing agents, for instance, metal chlorides.[17–21]

Thermogravimetric analysis (TGA) is an efficient way to assess the potential of boron- and nitrogen-containing materials, provided the data available in the open literature are taken into account. Advantageously, the thermogravimetric analyzer is easy to use, enables reproducible measurements (provided regular calibrations are performed) as well as satisfactory reproduction of results reported in the literature, and can be fast (depending on the heating rate and the final temperature of analysis). Accordingly, and on the basis of our experience with the chemistry of boron- and/or nitrogen-containing materials, we chose to routinely use TGA for screening new compounds and for assessing, by comparison with the data obtained with a pristine borane, the destabilization effect of destabilizing agent(s). This is the main topic of the present work. Several metal (II) chlorides (MCl_2) were screened as destabilizing agents of solid-state hydrazine borane, with the objectives of (i) showing that TGA is a highly efficient analytical tool for a fast and reliable selection of materials (in the present case, for chemical hydrogen storage) and (ii) proposing an efficient couple of metal chlorides (e.g., $CuCl_2$–$NiCl_2$) for the destabilization of hydrazine borane to be investigated more deeply in a further step.

2. Results and discussion

2.1. TGA-DTG data of HB@Cu

Hydrazine borane in pristine state has been reported to be unsuitable for solid-state chemical hydrogen storage.[7] Under heating (5 °C min^{-1}), it melts at about 60 °C and concomitantly decomposes with evolution of pure hydrogen (1.2 wt% H_2 at 95 °C). At 105–160 °C, an important mass loss (28.7 wt%) takes place because of the liberation of great amounts of hydrazine N_2H_4 in parallel to hydrogen. Then the solid residue appears to be rather stable up to about 250 °C, the temperature at which there is a mass loss of 4.3 wt% consisting of pure hydrogen. Note that the solid residue recovered upon heating up to 350 °C is shock-sensitive. The reaction mechanisms are rather unknown.[7–16] It is assumed that hydrogen forms by intermolecular reactions between $H^{\delta-}$ and $H^{\delta+}$ of hydrazine borane molecules followed by dehydropolymerization and/or dehydrocyclization of the $N_2H_3BH_2$ entities; the liberation of hydrazine is explained by reaction of the BH_3 group of one hydrazine borane molecule with another one, resulting in disruption of the B–N dative bond of the first molecule with liberation of hydrazine. More details are available elsewhere.[7,8]

Because $CuCl_2$ is the most efficient dopant in thermolysis of ammonia borane,[18–21] it was chosen in the first step as the main dopant of hydrazine borane. However, in the present work, 3 wt% $CuCl_2$ (denoted **HB@Cu**) appeared to be less efficient for destabilizing hydrazine borane. Compared to pristine hydrazine borane, the TGA-DTG profiles are quite similar (Figures 1a and 1b). The mass losses at 200 °C are close, the difference being 0.6 wt%, which is quite similar to the difference due to the weight of $CuCl_2$ (i.e. 0.5 wt%). There is a positive effect, with a shift of the low weight loss taking place at <100 °C. In the presence of $CuCl_2$, it starts at about 55 °C and 1.2 wt% of products are evacuated. Accordingly, it was decided to combine $CuCl_2$ with another metal (II) chloride MCl_2 in order to screen possible effects of the second dopant. Combination of two metal (II) chlorides was envisaged because, as reported below, higher destabilization than with a single metal (II) chloride was observed (a first possible reason of such positive effect could be stress in the lattice of the metal (II) chlorides).

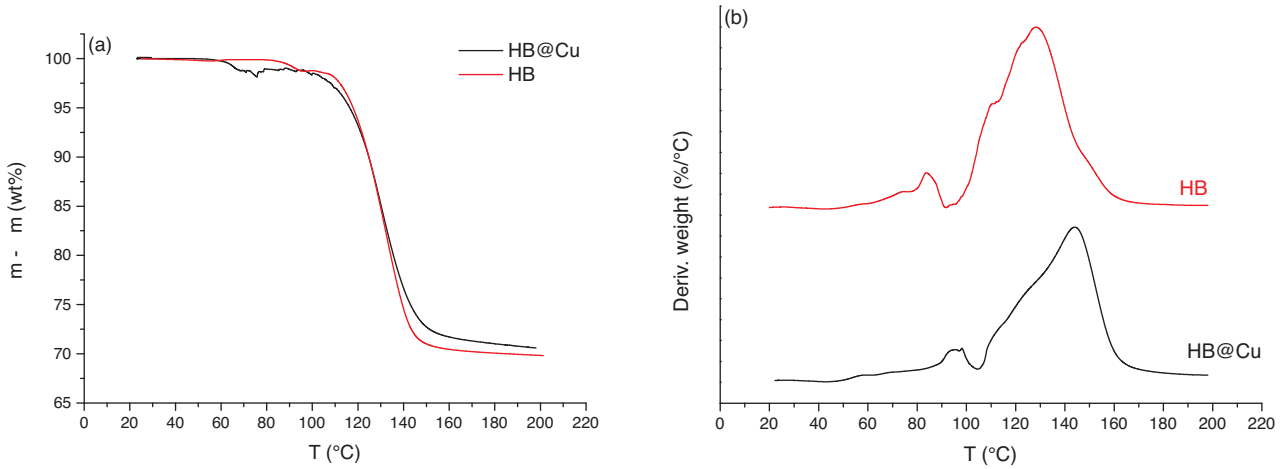

Figure 1. (a) TGA and (b) DTG results of **HB** and **HB@Cu.**

Compared to the destabilization of ammonia borane (NH_3BH_3) by $CuCl_2$, the TGA-DTG results obtained with **HB@Cu** are very different. The affinity of $CuCl_2$ with the borane would be dependent on the nature of the NH_3/N_2H_4 group and/or the strength of the B–N bond. It was suggested that the destabilization of ammonia borane is due to Lewis acid–base interactions between the metal cation M^{2+} and the B–N bond, and then formation of germs $M^{2+} \cdots N(H_2)–BH_2$ concomitantly with the generation of H_2. The best destabilization effects were observed with $CuCl_2$, followed by $CoCl_2$, $FeCl_2$, $NiCl_2$, and $PtCl_2$.[20] The present TGA-DTG results (Figures 1a and 1b) indicate that $CuCl_2$ has less affinity with hydrazine borane.

Of note is the "noise" that can be seen after the first mass loss on the TGA curve of **HB@Cu** (Figure 1a). This is due to the melting of the borane and subsequent generation of gas that leads to foaming and perturbations of the weight measurements.[7,22]

2.2. TGA-DTG data of HB@Cu-M

Two sets of metal (II) chlorides were considered: (i) 3d-metal (II) chlorides like $FeCl_2$, $CoCl_2$, and $NiCl_2$, where the metals have Pauling electronegativity of 1.8–1.9; and (ii) d^8-metal chlorides like $NiCl_2$, $PdCl_2$, and $PtCl_2$, where the Pauling electronegativity of Pd and Pt is slightly higher (2.2 and 2.28, respectively). $CuCl_2$ and one of these MCl_2 were mixed together (equimolar amounts), and added to hydrazine borane to get an overall loading of 3 wt%. The mixture-doped hydrazine borane samples are denoted **HB@Cu-M** with M as Fe, Co, Ni, Pd, and Pt. The mole number of the chlorides anions is similar for all of the samples.

Figures 2a and 2b show the TGA-DTG results for **HB@Cu-M** with M as Fe, Co, and Ni. The presence of the second metal chloride is positive, the effects being different from one salt to the other. The TGA-DTG profiles highlight four main observations. (1) The most important effect in terms of onset temperature of decomposition, when only the most important mass loss is considered, is achieved with $NiCl_2$ (32 °C), followed by $FeCl_2$ (45 °C) and $CoCl_2$ (50 °C). With respect to **HB@Cu-Fe**, the derivation curve suggests a first small decomposition at ca. 30 °C, but it may be neglected. (2) The DTG profiles are more or less different and complex, being constituted of at least 3 distinguishable signals. The main decomposition of the borane, which is roughly decomposed into two overlapping steps, peaks at 45, 53, and 95 °C for **HB@Cu-Ni**, **HB@Cu-Fe**, and **HB@Cu-Co**, respectively. These observations suggest that the destabilization takes place

in a different way depending on the second metal (II) chloride. (3) The decomposition extent at 100 °C is much higher than that reported for pristine hydrazine borane (1.5 wt%), with 17.7, 16.5, and 11.4 wt% for **HB@Cu-Fe**, **HB@Cu-Ni**, and **HB@Cu-Co**, respectively. This is indicative of the important destabilization effect occurring in the presence of the mixtures of metal (II) chlorides. (4) The decomposition extent at 200 °C is lower than that reported for pristine hydrazine borane (30.2 wt%), with 22.5, 24.2, and 26.5 wt% for **HB@Cu-Fe**, **HB@Cu-Ni**, and **HB@Cu-Co**, respectively. Such decreases were also reported for several metal chloride-doped ammonia borane samples; they were attributed to a mitigated release of unwanted gaseous by-products (mainly borazine).[18–21] Similar consequences may be assumed to occur with the present metal (II) chlorides-doped hydrazine borane samples (note that the analysis of the by-product N_2H_4 is difficult by TGA-MS; cf. section 3 for more details). We thus suggest that the metal (II) chlorides have a positive effect on mitigating the release of unwanted by-products; however, their effect is not positive enough since the mass loss is higher than the hydrogen content of hydrazine borane in the samples (i.e. 14.9 wt%). The release of hydrazine as the main by-product is likely,[7,9,12,13,15] but the formation and evolution of other by-products (e.g., ammonia NH_3, diborane B_2H_6, compounds with B–Cl bonds) cannot be discarded.

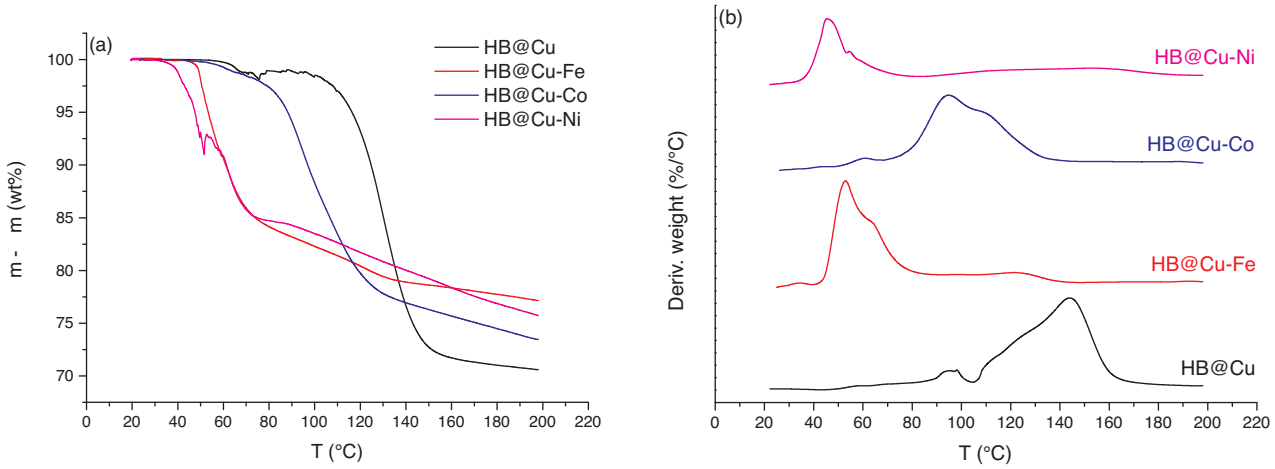

Figure 2. (a) TGA and (b) DTG results of **HB@Cu-Fe**, **HB@Cu-Co**, and **HB@Cu-Ni.** For comparison, the TGA-DTG results of **HB@Cu** are also given.

Figures 3a and 3b show the TGA-DTG results for **HB@Cu-M** with M as Ni, Pd, and Pt. Like the previous samples, the presence of the second metal (II) chloride is positive, the effects being different from one salt to the other. The comparison of these profiles highlights four main observations. They are equivalent to those reported in the previous paragraph. (1) The most important effect in term of onset temperature of decomposition is achieved by $NiCl_2$ (32 °C), followed by $PtCl_2$ (35 °C) and $PdCl_2$ (42 °C). (2) The TGA-DTG profiles are different, depending on the second metal (II) chloride. (3) The decomposition extent at 100 °C is as follows: 16.5, 14.4, and 10.1 wt% for **HB@Cu-Ni**, **HB@Cu-Pd**, and **HB@Cu-Pt,** respectively. The TGA-DTG profile of **HB@Cu-Pd** resembles that of **HB@Cu**; it is shifted to lower temperatures and lower mass losses. With respect to the TGA profile of **HB@Cu-Pt**, it is different from the others, with two successive mass losses at 25–55 °C and an almost linear one at >55 °C. (4) The decomposition extent at 200 °C is as follows: 24.2, 23.4, and 22.8 wt% for **HB@Cu-Ni**, **HB@Cu-Pd**, and **HB@Cu-Pt**, respectively.

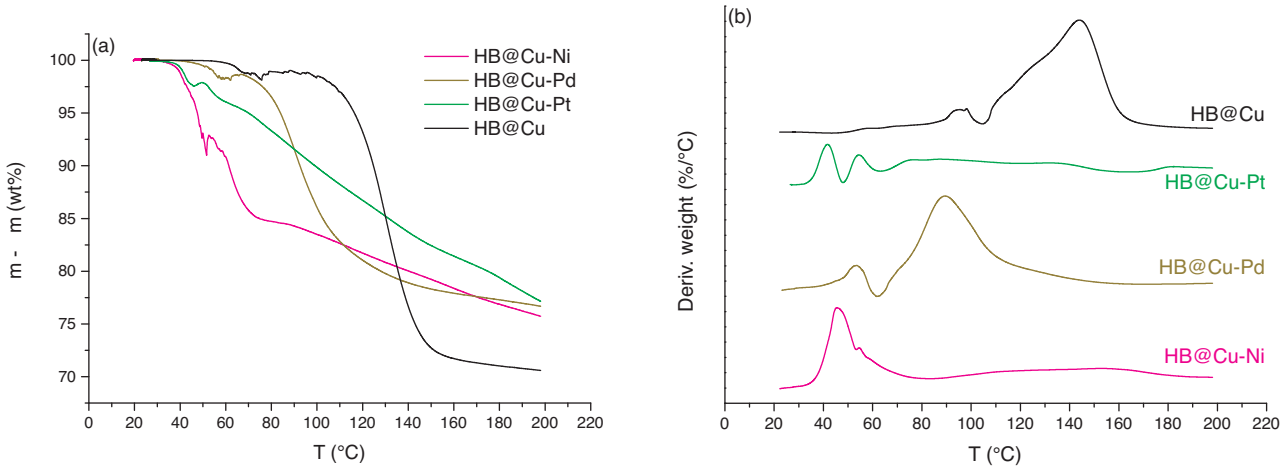

Figure 3. (a) TGA and (b) DTG results of **HB@Cu-Pd** and **HB@Cu-Pt.** For comparison, the TGA-DTG results of and **HB@Cu-Ni** and **HB@Cu** are also given.

To finalize the screening, the TGA-DTG profiles (Figures 2a, 2b, 3a, and 3b) can be compared while taking into account three criteria: namely, (i) the onset temperature of decomposition; (ii) the mass loss at <100 °C; and (iii) the overall mass loss at 200 °C. The following classification stands out: **HB@Cu-Ni** > **HB@Cu-Pt** > **HB@Cu-Fe** > **HB@Cu-Pd** > **HB@Cu-Co**. Then **HB@Cu-Ni** was selected for further screening.

2.3. Further exploitation of the TGA-DTG data of HB@Cu-M

Of note is the exploration of a possible correlation between the properties of the metal (II) chlorides/metals and some selected TGA-DTG data. The following properties were considered: for MCl_2, melting point, heat of formation, and lattice energy; for M^{2+} and/or M, the Pauling electronegativity, the electron affinity, the d-band center,[23] the ionic radius, and the redox potential. The following TGA-DTG data were considered: for the first main decomposition, onset temperature, DTG peak temperature, and mass loss after the decomposition; mass loss at 100 °C; and mass loss at 200 °C. These data were plotted as a function of the properties while taking into account only the second metal (II) chloride (for **HB@Cu**, it was assumed that the second metal (II) chloride was half of $CuCl_2$). Trends were observed in a few cases.

Figures 4a–4d show four curves as a function of the redox potential. Firstly, if the data relative to **HB@Cu-Ni** are neglected, volcano-shape variations peaking for $E^\circ(Cu^{2+}/Cu) = 0.337$ V vs. SHE can be observed. The copper-based dopant would have the least suitable redox properties for the destabilization of hydrazine borane. Secondly, if the data relative to **HB@Cu-Ni** are taken into consideration, there is no specific trend anymore. For example, the potentials $E^\circ(Ni^{2+}/Ni)$ and $E^\circ(Pt^{2+}/Pt)$ are very different, with –0.23 and +1.2 V vs. SHE, but the reported destabilization properties are equivalent. Another interesting point is that the reduction of Pd^{2+} and Pt^{2+} by in-situ formed H_2 may also occur, leading to the formation of H^+ that may readily react with the BH_x moieties. This may rationalize the different TGA-DTG profiles for **HB@Cu-Pd** and **HB@Cu-Pt**.

There is no trend with the d-band center of the metals. Nevertheless, copper has the lowest d-band center with –2.67 eV (vs. –2.25 eV for Pt, –1.83 eV for Pd, –1.29 eV for Ni, –1.17 eV for Co, and –0.92 eV for Fe),[22] and also the least good TGA-DTG results. In fact, the behavior of copper toward hydrogen is closer to that of

gold than to that of platinum.[24,25] These facts suggest that the electronic properties of copper would not be appropriate for the destabilization of hydrazine borane via interactions with the hydrogen atoms.

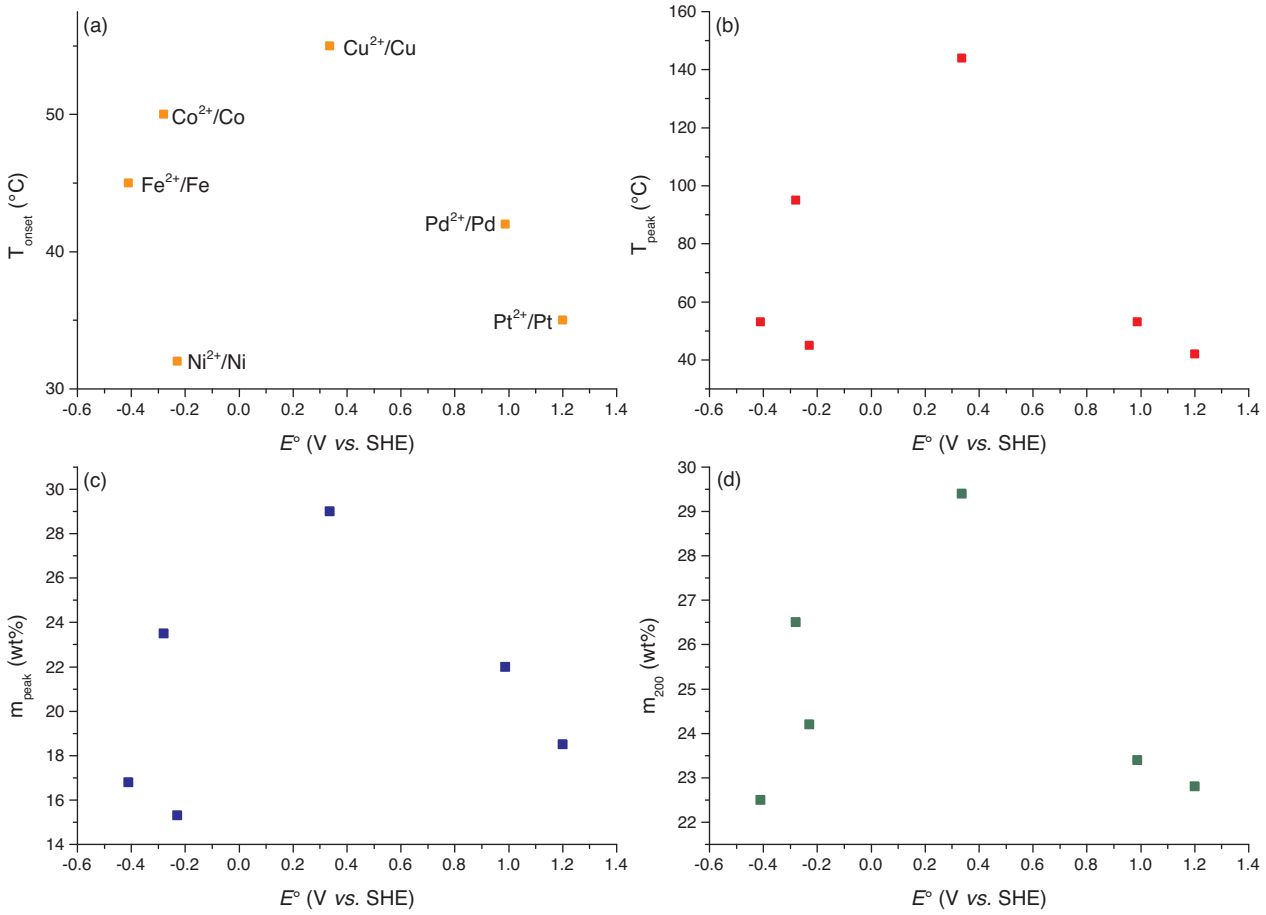

Figure 4. Evolution of results from the TGA-DTG experiments as a function of redox potentials (E° in V vs. SHE). (a) Onset temperature of the first main decomposition (T_{onset} in °C). (b) DTG peak temperature of the first main decomposition (T_{peak} in °C). (c) Mass loss after the first main decomposition (Δm_{peak} in wt%). (d) Overall mass loss at 200 °C (Δm_{200} in wt%).

The metal (II) chlorides $FeCl_2$, $CoCl_2$, and $NiCl_2$ were selected because they are neighboring 3d-metals. The difference in effect in the destabilization of hydrazine borane (Figure 2a) may be explained by the electronic structure of the metal cations: Fe^{2+} s^1d^5; Co^{2+} s^2d^5; Ni^{2+} s^2d^6. The most stable configuration is that of Co^{2+}, followed by Fe^{2+} and Ni^{2+}. This is in agreement with the ranking proposed in the previous section. The metal (II) chlorides $NiCl_2$, $PdCl_2$, and $PtCl_2$ were selected because they are composed of d^8-metals, with similar electronic structures for M^{2+} (s^2d^6). Figures 5a–5d show four trends for these metals. These correlations suggest that both electronic and geometric effects may account for the destabilization of hydrazine borane. The electronic effects would drive the decomposition extent. Stronger interactions would take place with the noble metals, likely hindering the formation of the unwanted hydrazine. The geometric effects would drive the reactivity at low temperatures. The higher the ionic radius is (e.g., for Pd^{2+}), the higher the onset temperature for the first main decomposition. This explains why the onset is higher with **HB@Cu-Pd**.

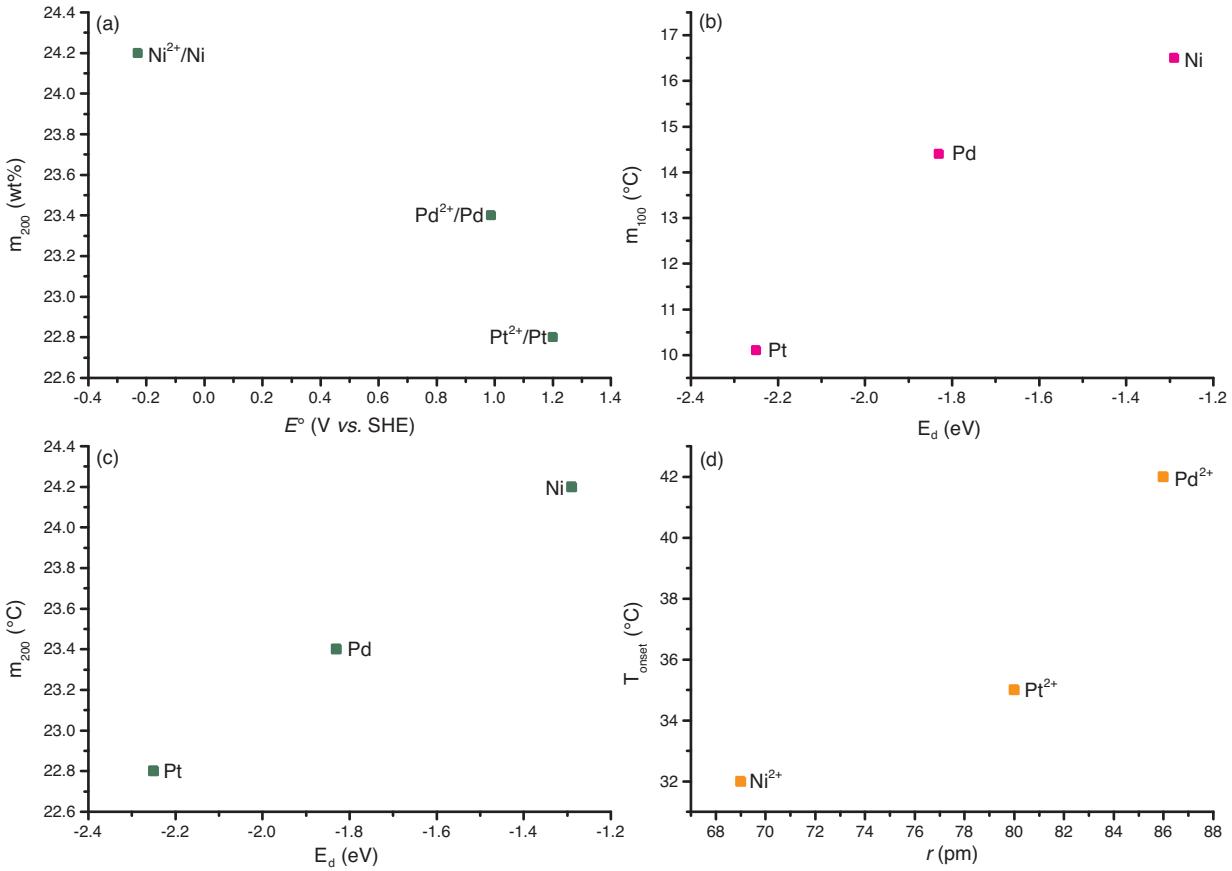

Figure 5. (a) Evolution of the overall mass loss at 200 °C (Δm_{200} in wt%) as a function of redox potentials of M^{2+}/M (E° in V *vs.* SHE). (b) Evolution of the mass loss at 100 °C (Δm_{100} in wt%) as a function of the d-band centers (ε_d in eV) of Pt, Pd, and Ni. (c) Evolution of the overall mass loss at 200 °C (Δm_{200} in wt%) as a function of the d-band centers (ε_d in eV). (d) Evolution of the onset temperature of the first main decomposition (T_{onset} in °C) as a function of the ionic radius (r in pm) of M^{2+}.

The classification proposed in the previous section is somehow the reverse of that proposed for the metal (II) chloride-doped ammonia borane. With ammonia borane, the classification was as follows: $CuCl_2 \sim CoCl_2 > FeCl_2 > NiCl_2 > PtCl_2$. It was proposed that copper offers optimal doping activity with intermediate binding energies, enabling weak binding to H, adequate (optimal) binding with N of NH_3BH_3, and formation of H_2 and the germ $Cu^{2+}\cdots N(H_2)$–BH_2 (preceded by interaction between the metal cation and the dative bond).[20] With hydrazine borane and the presence of the N_2H_4 moiety, copper would not have the optimized properties. Due to steric hindrance, the central NH_2 of $N_2H_4BH_3$ is accessible mainly through $M^{2+}\cdots H$ interactions, which is favored with metals showing strong affinity with H like Ni and Pt. The terminal NH_2 of $N_2H_4BH_3$ is accessible to the metal cations through $M^{2+}\cdots N$ interactions (via the lone pair of N), but the destabilization of the BH_3 moiety via the B–N bond should be less important than for ammonia borane. This may explain why the destabilization of hydrazine borane by $CuCl_2$ and $CoCl_2$ is weaker than that of ammonia borane.[20] It is thus suggested that the destabilization of hydrazine borane by MCl_2 is driven by $M^{2+}\cdots H$–$N(H)(NH_2)$–BH_3 interactions between M^{2+} and the hydrogens of the central NH_2. The metals with high affinity with hydrogen are thus more effective dopants.

2.4. TGA-DTG data of *x*HB@Cu-Ni

The loading x of $CuCl_2$-$NiCl_2$ (equimolar mixture) was varied from 1 to 10 wt%. The samples are denoted ***x*HB@Cu-Ni**. For these samples, the hydrogen content, taking into account the weight of the metal (II) chlorides, varies from 15.15 to 13.8 wt%. Figures 6a and 6b show the TGA-DTG results.

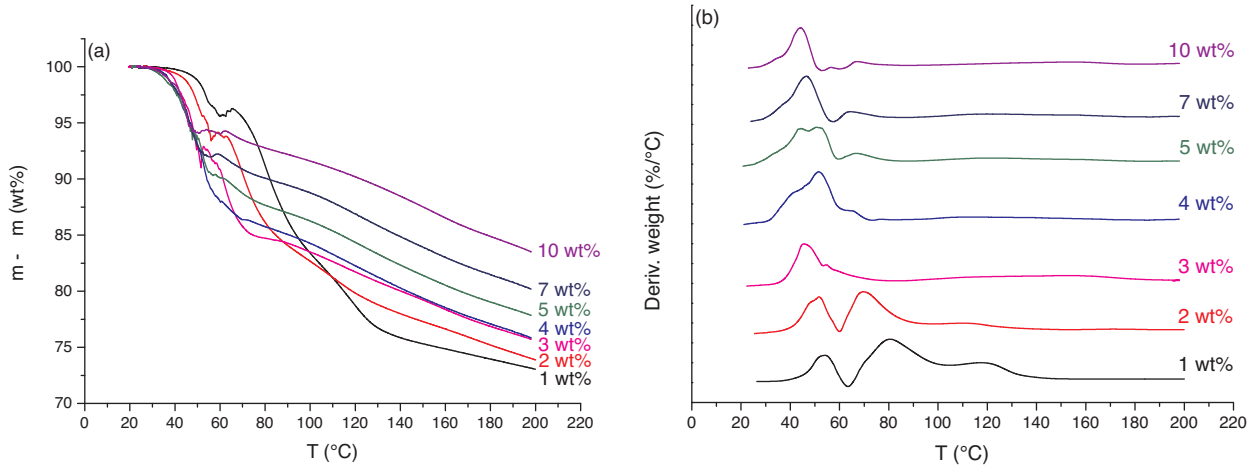

Figure 6. (a) TGA and (b) DTG results of ***x*HB@Cu-Ni**, with ***x*** varying from 1 to 10 wt%.

In solid state, the reaction of the metal (II) chlorides with hydrazine borane should occur via grain-to-grain contacts. Direct destabilization would then be driven by a limited amount of hydrazine borane molecules, especially those at the surface of the crystallites in contact with the MCl_2 grains. The destabilized surface entities are expected to destabilize neighbor molecules by chain reaction.[18,19] The TGA-DTG results are evidence of that. A first observation is that, by increasing the loading from 1 to 4 wt%, the onset temperature of decomposition is lowered from 37 to 30 °C. The more the MCl_2 grains are, the higher the number of contacts between MCl_2 and HB grains. However, by further increasing the loading up to 10 wt%, the effect on the onset temperature of decomposition can be neglected, being constant at around 30 °C.

In a first approximation, it can be stated that over the range 20–100 °C there are roughly 2 main decompositions. For the loadings 1 and 2 wt%, they are separated, but for a loading of 3 wt% and higher, they are overlapped. Without approximation, the decomposition appears to be quite complex, with several minor/major overlapping steps. With the increase in the loading, the overall decomposition tends to be uniform. This is especially the case for the loadings 4-10 wt%. Few complementary observations stand out. With respect to the first mass loss, it increases with the loading from 1 to 4 wt%, but then decreases when the loading is further increased. The evolution of the mass loss as a function of the loading has a Λ-shape (Figure 7a). With respect to the second mass loss, it significantly and linearly decreases with the increase in the loading from 1 to 4 wt%, but at higher loadings the decrease is less pronounced (Figure 7b). These trends are consistent with our previous discussion concerning the grain-to-grain contacts.

For the samples with a loading of 2 to 10 wt%, the time evolution of the mass loss after the initial main decompositions is almost parallel. This is particularly obvious for **10HB@Cu-Ni** and **7HB@Cu-Ni** from ca. 60 °C, **5HB@Cu-Ni** from ca. 70 °C, **4HB@Cu-Ni** from ca. 80 °C, **3HB@Cu-Ni** from ca. 100 °C, and **2HB@Cu-Ni** from ca. 120 °C. This is indicative of similar mechanisms of decomposition, maybe that of the polymeric residue $\mathbf{BN}_y\mathbf{H}_z$ ($y < 2$ and $z < 7$)[7] forming upon the initial main decompositions. For

the decomposition of $\mathbf{BN_yH_z}$, the dopants (in reduced form M^0 or $M^{\alpha+}$ with $\alpha < 2$)[18–21] may have no or only small effect. This was also reported for the second decomposition of ammonia borane by bimetallic NiPt systems.[26]

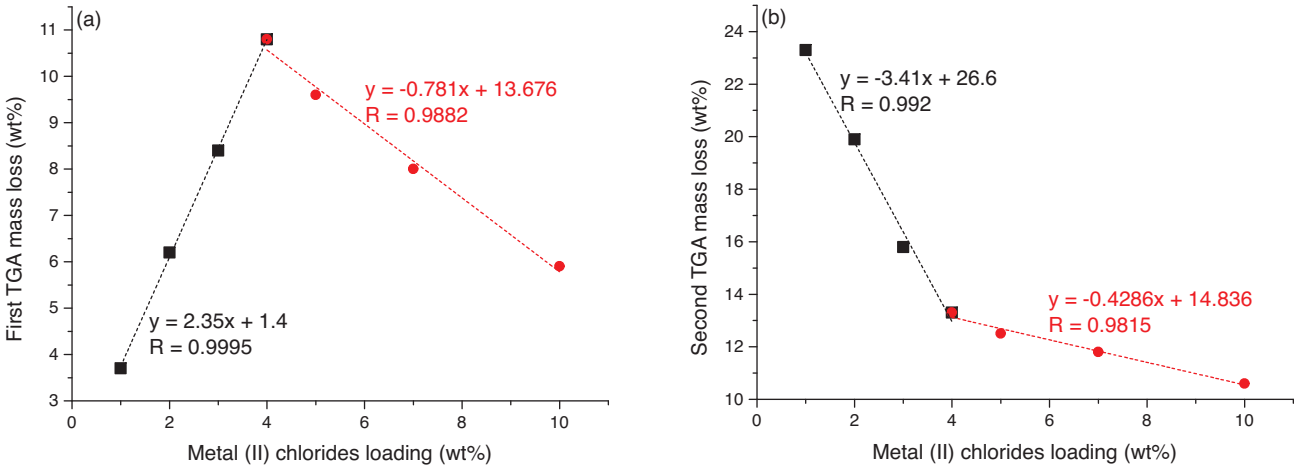

Figure 7. Evolution of (a) the first mass and (b) second mass losses from the TGA data (Figure 6a) as a function of the metal (II) chlorides loading for **HB@Cu-Ni**.

The overall mass loss at 200 °C decreases from 27 to 16.5 wt% with the increase in the loading from 1 to 10 wt% (Figure 8). The decrease is linear, with a slope of –1.04 ($R^2 = 0.9874$). This is in agreement with the aforementioned grain-to-grain destabilization effect. The higher the amount of metal (II) chlorides is, the more the contact between the grains, and thus the better the effect on the destabilization properties of the borane. Compared to the theoretical gravimetric hydrogen density of ***x*HB@Cu-Ni** reported in Figure 8, the mass losses are higher but lower than for pristine hydrazine borane. Furthermore, the increase in the loading leads to less mass loss, suggesting a more important mitigation of the evolving by-products.

2.5. TGA-DTG data of 3HB@Cu$_a$-Ni$_{100-a}$

The molar proportion of $CuCl_2$ and $NiCl_2$ (for an overall loading of 3 wt%) was varied. Samples with the following molar percentages ***a*** were prepared: 100, 90, 70, 50, 30, 10, and 0. The samples are denoted **3HB@Cu$_a$-Ni$_{100-a}$**, except those containing only $CuCl_2$ (**3HB@Cu**) or $NiCl_2$ (**3HB@Ni**). Figures 9a and 9b show the TGA-DTG results (25–200 °C, 5 °C min^{-1}).

As a first observation, one may focus on the TGA-DTG curves obtained with **3HB@Ni**. Doping hydrazine borane with $NiCl_2$ is beneficial. The onset temperature of decomposition of hydrazine borane is as low as 34 °C. There is roughly a main decomposition (34–75 °C), consisting of two overlapping/successive steps. The mass loss at 75 °C is 14 wt%. The overall mass loss at 200 °C is 23.6 wt%. A positive destabilization effect of nickel chloride was also reported for ammonia borane.[22] Compared to **3HB@Cu**, the results are better. Hence, the **3HB@Ni** could be preferred for future destabilization works.

Much better decomposition results are obtained when both $CuCl_2$ and $NiCl_2$ are present. (1) The onset temperature of decomposition is decreased, e.g., to 28 °C for **3HB@Cu$_{70}$-Ni$_{30}$**. (2) The decomposition extent at 200 °C is lowered, with, e.g., 18.7 wt% for **3HB@Cu$_{10}$-Ni$_{90}$**. (3) A careful analysis of the TGA-DTG

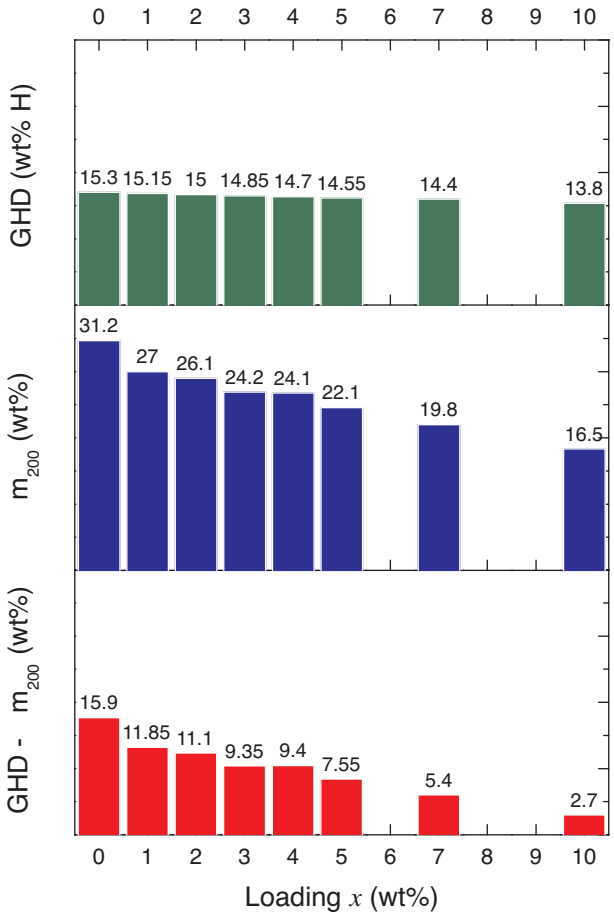

Figure 8. Comparison of the theoretical gravimetric hydrogen density (GHD in wt%) of ***x*HB@Cu-Ni** with the mass loss (Δm_{200} in wt%) at 200 °C from the TGA data in Figure 6a, and difference between these values, for each of the ***x*HB@Cu-Ni** samples (with x the loading in metal (II) chlorides in wt%).

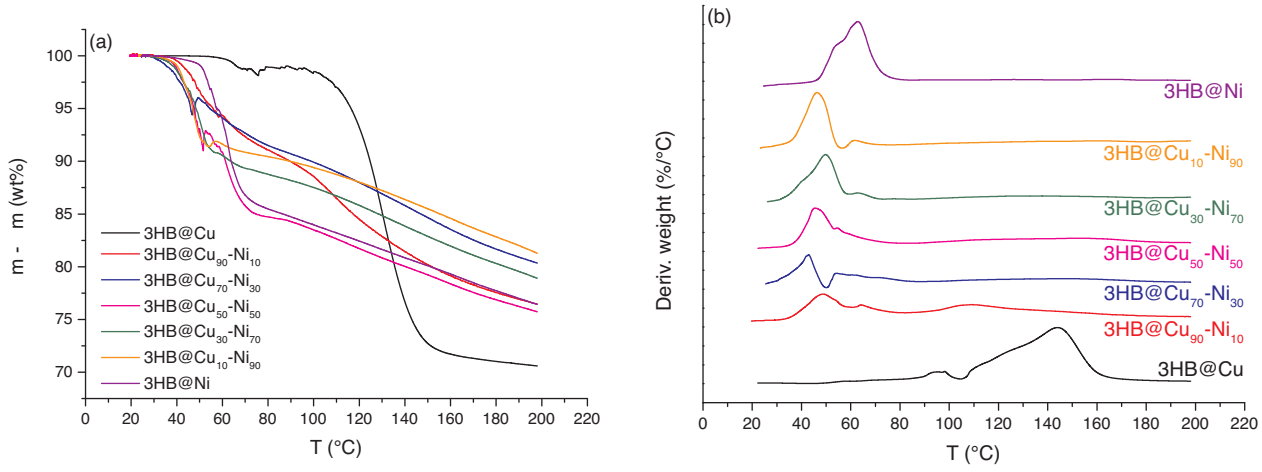

Figure 9. (a) TGA and (b) DTG results of **3HB@Cu$_a$-Ni$_{100-a}$** with ***a*** (in mol%) varying from 0% to 100%.

data (onset temperature and mass losses) does not reveal trends. (4) Nevertheless, the profile obtained with **3HB@Cu$_{10}$-Ni$_{90}$** seems to be the most interesting, with an onset temperature of 29 °C, a first mass loss of 8.6 wt% at 55 °C, and an overall mass loss of 18.7 wt% at 200 °C. By DSC (not reported), the enthalpy of the first decomposition (peaking at 51 °C) was measured as being 29.2 kJ mol^{-1} $N_2H_4BH_3$ and that of the second one (peaking at 129 °C) was found to be 2 kJ mol^{-1} $N_2H_4BH_3$. No melting was evidenced for this sample. In comparison to pristine hydrazine borane,[7] the first enthalpy is higher of 9 kJ mol^{-1} $N_2H_4BH_3$, and the second decomposition is not observed with the unloaded sample. These observations suggest different decomposition paths for **3HB@Cu$_{10}$-Ni$_{90}$**.

3. Discussion

Studying doped boron- and nitrogen-containing materials is difficult from a technical point of view because of (i) sensitivity to moisture and air, (ii) risk of decomposition at low temperatures (30–50 °C), and (iii) high reactivity towards acids and oxidants. Studying the solid residues recovered after decomposition (at, e.g., 200 °C) is also difficult from a technical point of view because of (i) amorphous state, (ii) insolubility in aprotic solvents, (iii) sensitivity to moisture and air, and in a few cases (iv) instability/shock-sensitivity.[1–3] Analyzing the main by-product (i.e. N_2H_4) stemming from the thermolytic decomposition of hydrazine borane is difficult because of condensation (bp 114 °C) onto any cold wall between the TGA apparatus and the MS device.[7,9,13,15] Consequently, characterizing fresh/decomposed boron- and nitrogen-containing materials is difficult by, e.g., XRD, MAS NMR, FTIR, ICP-AES, SEM, and EDX.

Indeed, the loading of the metal (II) chlorides is too low to get visible diffraction peaks in the midst of the numerous peaks of hydrazine borane. By FTIR, the spectra of the freshly mixed samples are identical to that of pristine hydrazine borane. However, both analyses suggest no evolution or negligible change in the borane when put into contact with the chlorides. Solid-state ^{11}B MAS NMR spectroscopy experiments on the fresh samples have to be avoided for safety and technological reasons. The doped samples are unstable at temperatures as low as 30 °C. There is thus a risk of decomposition during high-speed rotation of the NMR sample holder. Furthermore, the collected data would not be exploitable because of in-situ evolution of the signal of the BH_3 group and apparition of new ones due to BH_x environments (indicating the decomposition of the borane). The reactivity of hydrazine borane (strong reducing agent) and its destabilization by the metal (II) chlorides impede the use of ICP-AES and EDX spectroscopy. With the former technique, the sample has first to be mineralized with the help of concentrated acids, which leads to fast, even explosive, generation of H_2. With the latter one, the samples may decompose under vacuum and the boranes are not stable under the electron beam. In fact, techniques using vacuum and/or electron beam are not appropriate for this kind of sample.

In this context, we developed a methodology based on TGA to screen boron- and nitrogen-containing materials, including new compounds, composites made of two hydrides, nanoconfined boranes, and doped ammonia/hydrazine boranes. The TGA profiles allow screening and classifying the destabilized samples, verifying the presence of dopants (or that of impurity in any freshly synthesized borane), assessing if the borane had evolved during the preparation of the mixture, and anticipating about the evolution of gaseous by-products. In addition, DTG provides the decomposition rate and the DTG peak temperature can be used as a characteristic value to specify an appropriate step. To a certain extent, TGA-DTG replaces the aforementioned techniques. The present work is an illustration of that. The protocol proposed for the TGA-DTG experiments could be used by other groups involved in the field so that comparisons of data from different published studies are relevant.

It is important to mention that TGA also helps in discarding any unstable or too reactive materials, given that any event (e.g., explosion under inert atmosphere) is limited by the small amounts used in our conditions (<2 mg). By contrast, provided small amounts are used, TGA enables a first screening of compounds that could have potential as energetic materials (for propulsion).

The TGA-DTG results described above highlight four main comments. (1) Unlike for ammonia borane, $CuCl_2$ is not a dopant of choice to destabilize hydrazine borane, and unlike ammonia borane, $NiCl_2$ is preferable. This suggests that interactions between M^{2+} and the boranes are different. For ammonia borane, $Cu^{2+} \cdots N$ interactions drive the destabilization of the compound by weakening the B–N dative bond. For hydrazine borane, $Ni^{2+} \cdots H$ interactions would drive the destabilization of the material and nickel is known to have better affinity towards hydrogen than copper. $Cu^{2+} \cdots N$ interactions with the lone pair of the terminal NH_2 of hydrazine borane would not be strong enough to destabilize the B–N bond in longer range. Further works are now required to confirm this assumption. (2) The presence of both $CuCl_2$ and $NiCl_2$ is beneficial to the destabilization of hydrazine borane in terms of onset temperature of decomposition, mass loss at 100 °C, overall mass loss at 200 °C, and amount of evolving by-products. The addition of some $CuCl_2$ has a synergetic effect on the action of $NiCl_2$. It is thus suggested that the sample **3HB@Cu$_{10}$-Ni$_{90}$** is worth being studied more. (3) In solid state, the reaction of the metal (II) chlorides with hydrazine borane occurs via grain-to-grain contacts, as evidenced by the improved decomposition properties with the increase in the loading of $CuCl_2$-$NiCl_2$ up to 10 wt%. This has also a positive effect on the amount of by-products, which likely decreases. (4) The destabilization may be also explained in terms of geometric effects, especially for $PdCl_2$, whose ionic radius is bigger than that of Ni^{2+} and Pt^{2+}. Smaller radii would improve the destabilization of hydrazine borane.

A last remark can be made on the basis of the present TGA-DTG results and those reported for doped ammonia borane in a previous work.[20] Assuming the occurrence of different $M^{2+} \cdots X$ (with M the metals studied herein, and X = H or N) depending on the nature of the N-based moiety (e.g., NH_3 vs. N_2H_4, and also NH_2, N_2H_3, etc.), the boron- and nitrogen-containing materials could be valorized as reducing agents of different strengths in organic chemistry (e.g., conversion of –C=O to –C–OH) and for the synthesis of metallic nanoparticles.

In the present study, the primary intention was to illustrate the importance of TGA as a preliminary analysis technique and as a screening method for a first exploration of the potential of boron- and nitrogen-containing materials for chemical hydrogen storage. To this end, and for the first time, the effect of metal (II) chlorides on the destabilization of hydrazine borane ($N_2H_4BH_3$) was considered. Relevantly chosen metal (II) chlorides (MCl_2) (with M as four neighboring 3d-metals and as three d^8-metals) were selected. Screening these metal (II) chlorides as dopants of hydrazine borane was the secondary goal of the work. Careful scrutiny of the TGA-DTG curves suggested several items of information. The most important ones are as follows: (1) Copper chloride is inefficient in destabilizing hydrazine borane via interactions between Cu^{2+} and the B–N bond, which was explained by the steric hindrance due to the N_2H_4 moiety. In contrast, nickel chloride is efficient in destabilizing hydrazine borane owing to its strong affinity with hydrogen and the likely occurrence of $Ni^{2+} \cdots H$ interactions, with H of the central NH_2 of the molecule. (2) The destabilization of the borane is more important when both chlorides are combined. The decomposition takes place from temperatures as low as ca. 30 °C (vs. 81 °C for pristine hydrazine borane). (3) When both chlorides (in equimolar amounts) are loaded at 10 wt%, the amount of evolving by-products is decreased. (4) The most efficient destabilizing composition is proposed to be 3 wt% $CuCl_2$-$NiCl_2$, where the $NiCl_2$ content is 90 mol%. It is thus suggested

to focus on this sample, as well as on 3 wt% $NiCl_2$-doped hydrazine borane, in future works. The reported TGA-DTG-based results highlighted the possibility to destabilize hydrazine borane with d^8-metal chlorides (halides and other salts could be also envisaged), go further with two of the screened samples to improve the dehydrogenation properties for the prospect of chemical hydrogen storage, envisage a few samples as energetic materials (for propulsion and fast H_2 generation systems), and explore the reducing properties of hydrazine borane for synthesis of mono-/bimetallic nanoparticles. Above all, the present report shows the importance of TGA in the field of boron- and nitrogen-containing materials, and the proposed TGA protocol could be used by other groups so that literature-based data comparisons are more relevant.

4. Experimental

Hydrazine borane was prepared according to an optimized procedure reported in detail elsewhere.[7] Of purity >99%, it is stored and handled in an argon-filled glove box (MBraun M200B) where the oxygen and water contents are kept below 0.1 ppm. Several anhydrous metal (II) chlorides (MCl_2) were used as dopants/destabilizing agents: i.e. $FeCl_2$, $CoCl_2$, $NiCl_2$, and $CuCl_2$ as 3d-metal (II) chlorides; and $NiCl_2$, $PdCl_2$, and $PtCl_2$ as d^8-metal (II) chlorides. They were from Sigma-Aldrich or Strem Chemicals, stored in the glove box, and used as received. The preparation of the chloride-doped hydrazine borane was performed in the glove box according to a two-step procedure. The first step consisted of preparing the metal (II) chlorides mixture: $CuCl_2$ and MCl_2 in equimolar amounts or at the targeted mole percentages were weighed, mixed/ground gently together in a mortar, and then stored in a vial for quite-immediate use. The second step consisted of adding the as-prepared mixture to hydrazine borane: the former was first weighed, followed by the second one, and then mixed/ground gently together in a mortar;[18] finally, the freshly prepared mixture was loaded into the TGA crucible for analysis.

Thermogravimetric analysis (TGA) was performed on the analyzer Q500 from TA Instruments. Derivative thermogravimetric (DTG) analysis was deduced with the help of the tool of the software Universal Analysis. An aluminum crucible was used because it can be sealed in the glove box to protect the samples for oxidation and hydrolysis during the transfer from the glove box to the TGA apparatus. Typically, the crucible and the lid were first weighed by the TGA balance, and then transferred into the glove box. A mass between 2 and 3 mg of samples was placed in the crucible, which was then sealed with the lip by crimping. At the very last moment, before starting the analysis, the lid was pierced with a needle. In routine, i.e. for screening our samples, the following program was applied: temperature range 25–200 °C, heating rate 5 °C min^{-1}, N_2 flow rate 50 mL min^{-1}. Differential scanning calorimetry (2920 MDSC, TA Instruments; temperature range 25–200 °C, heating rate 5 °C min^{-1}, N_2 flow rate 50 mL min^{-1}) was used for the "best" sample, which was also analyzed by powder X-ray diffraction (Bruker D5005 powder diffractometer, equipped with CuKα radiation and $\lambda = 1.5406$ Å) and Fourier transform infrared spectroscopy (Nicolet 710).

Acknowledgments

Financial contributions from Centre National de la Recherche Scientifique (CNRS, France) and Direction Générale des Armées (DGA, France) are gratefully acknowledged.

References

1. Wang, P. *Dalton Trans.* **2012**, *41*, 4296–4302.
2. Moussa, G.; Moury, R.; Demirci, U. B.; Şener, T.; Miele, P. *Int. J. Energy Res.* **2013**, *37*, 825–842.
3. Jepsen, L. H.; Ley, M. B.; Lee, Y. S.; Cho, Y. W.; Dornheim, M.; Jensen, J. O.; Filinchuk, Y.; Jørgensen, J. E.; Besenbacher, F.; Jensen, T. R. *Mater. Today* **2014**, *17*, 129–135.
4. Hu, M. G.; Geanangel, R. A.; Wendlandt, W. W. *Thermochim. Acta* **1978**, *23*, 249–255.
5. Sit, V.; Geanangel, R. A.; Wendlandt, W. W. *Thermochim. Acta* **1987**, *113*, 379–382.
6. Baitalow, F.; Baumann, J.; Wolf, G.; Jaenicke-Rößler, K.; Leitner, G. *Thermochim. Acta* **2002**, *391*, 159–168.
7. Moury, R.; Moussa, G.; Demirci, U. B.; Hannauer, J.; Bernard, S.; Petit, E.; van der Lee, A.; Miele, P. *Phys. Chem. Chem. Phys.* **2012**, *14*, 1768–1777.
8. Goubeau, Von J.; Ricker, E. *Z. Anorg. All. Chem.* **1961**, *310*, 123–142.
9. Moury, R.; Demirci, U. B. *Energies* **2015**, *8*, 3118–3141.
10. Vinh-Son, N.; Swinnen, S.; Matus, M. H.; Nguyen, M. T.; Dixon, D. A. *Phys. Chem. Chem. Phys.* **2009**, *11*, 6339–6344.
11. Hügle, T.; Kühnel, M. F.; Lentz, D. *J. Am. Chem. Soc.* **2009**, *131*, 7444–7446.
12. Toche, F.; Chiriac, R.; Demirci, U. B.; Miele, P. *Int. J. Hydrogen Energy* **2014**, *39*, 9321–9329.
13. Petit, J. F.; Moussa, G.; Demirci, U. B.; Toche, F.; Chiriac, R.; Miele, P. *J. Hazard. Mater.* **2014**, *278*, 158–162.
14. Wu, H.; Zhou, W.; Pinkerton, F. E.; Udovic, T. J.; Yildirim, T.; Rush, J. J. *Energy Environ. Sci.* **2012**, *5*, 7531–7535.
15. Moury, R.; Demirci, U. B.; Ichikawa, T.; Filinchuk, Y.; Chiriac, R.; van der Lee, A.; Miele, P. *Chem. Sus. Chem.* **2013**, *6*, 667–673.
16. Chua, Y. S.; Pei, Q.; Ju, X.; Zhou, W.; Udovic, T. J.; Wu, G.; Xiong, Z.; Chen, P.; Wu, H. *J. Phys. Chem. C* **2014**, *118*, 11244–11251.
17. De Benedetto, S.; Carewska, M.; Cento, C.; Gislon, P.; Pasquali, M.; Scaccia, S.; Prosini, P. P. *Thermochim. Acta* **2006**, *441*, 184–190.
18. Benzoua, R.; Demirci, U. B.; Chiriac, R.; Toche, F.; Miele, P. *Thermochim. Acta* **2010**, *509*, 81–86.
19. Chiriac, R.; Toche, F.; Demirci, U. B.; Krol, O.; Miele, P. *Int. J. Hydrogen Energy* **2011**, *36*, 12955–12964.
20. Toche, F.; Chiriac, R.; Demirci, U. B.; Miele, P. *Int. J. Hydrogen Energy* **2012**, *37*, 6749–6755.
21. Chiriac, R.; Toche, F.; Demirci, U. B.; Miele, P. *Thermochim. Acta* **2013**, *567*, 100–106.
22. He, T.; Xiong, Z.; Wu, G.; Chu, H.; Wu, C.; Zhang, T.; Chen, P. *Chem. Mater.* **2009**, *21*, 2315–2318.
23. Hammer, B.; Nørskov, J. K. *Adv. Catal.* **2000**, *45*, 71–129.
24. Greeley, J.; Mavrikakis, M. *Nature Mater.* **2004**, *3*, 810–815.
25. Hammer, B. Nørskov, J. K. *Surf. Sci.* **1995**, *343*, 211–220.
26. Cheng, F.; Ma, H.; Li, Y.; Chen, J. *Inorg. Chem.* **2007**, *46*, 788–794.